Biometals (2012) 25:1061–1081
DOI 10.1007/s10534-012-9572-4

Biological and cytoselective anticancer properties of copper(II)-polypyridyl complexes modulated by auxiliary methylated glycine ligand

Hoi-Ling Seng · Wai-San Wang · Siew-Ming Kong · Han-Kiat Alan Ong · Yip-Foo Win · Raja Noor Zaliha Raja Abd. Rahman · Makoto Chikira · Weng-Kee Leong · Munirah Ahmad · Alan Soo-Beng Khoo · Chew-Hee Ng

Received: 14 January 2012 / Accepted: 10 July 2012 / Published online: 27 July 2012

Abstract A series of ternary copper(II)-1,10-phenanthroline complexes with glycine and methylated glycine derivatives, $[Cu(phen)(aa)(H_2O)]NO_3 \cdot xH_2O$ **1–4** (amino acid (aa): glycine (gly), **1**; DL-alanine (DL-ala), **2**; 2,2-dimethylglycine (C-dmg), **3**; sarcosine (sar), **4**), were synthesized and characterized by FTIR, elemental analysis, electrospray ionization–mass spectra (ESI–MS), UV–visible spectroscopy and molar conductivity measurement. The determined X-ray crystallographic structures of **2** and **3** show each to consist of distorted square pyramidal $[Cu(phen)(aa)(H_2O)]^+$ cation, a nitrate counter anion, and with or without lattice water, similar to previously reported structure of $[Cu(phen)(gly)(H_2O)]NO_3 \cdot 1½H_2O$. It is found that **1–4** exist as 1:1 electrolytes in aqueous solution, and the cationic copper(II) complexes are at least stable up to 24 h. Positive-ion ESI–MS spectra show existence of only undissociated $[Cu(phen)(aa)]^+$ species. Electron paramagnetic resonance, gel electrophoresis, fluorescence quenching, and restriction enzyme inhibition assay were used to study the binding interaction, binding affinity and selectivity of these complexes for various types of B-form DNA duplexes and G-quadruplex. All complexes can bind

Malaysian Patent No PI 2012700421.

Electronic supplementary material The online version of this article (doi:10.1007/s10534-012-9572-4) contains supplementary material, which is available to authorized users.

H.-L. Seng
Unit GL33, Malaysia University of Science and Technology, 47301 Petaling Jaya, Malaysia

W.-S. Wang · S.-M. Kong · Y.-F. Win · C.-H. Ng (✉)
Faculty of Science, Universiti Tunku Abdul Rahman, 3190 Kampar, Malaysia
e-mail: ngch@utar.edu.my

S.-M. Kong · M. Ahmad · A. S.-B. Khoo
Molecular Pathology Unit, Cancer Research Centre, Institute for Medical Research, 50588 Kuala Lumpur, Malaysia

H.-K. Alan Ong
Department of Pre-Clinical Sciences, Faculty of Medicine and Health Sciences, Universiti Tunku Abdul Rahman, 43000 Kajang, Malaysia

R. N. Z. Raja Abd. Rahman
Department of Microbiology, Faculty of Biotechnology and Biomolecular Sciences, Universiti Putra Malaysia, 43400 UPM Serdang, Selangor DE, Malaysia

M. Chikira
Department of Applied Chemistry, Chuo University, Kasuga 1-13-27 Bunkyo-ku, Tokyo 112-8551, Japan

W.-K. Leong
Division of Chemistry & Biological Chemistry, Nanyang Technological University, 21 Nanyang Avenue, SPMS-CBC-06-07, Singapore 637371, Singapore

selectively to DNA by intercalation and electrostatic forces, and inhibit topoisomerase I. The effect of the methyl substituents of the coordinated amino acid in the above complexes on these biological properties are presented and discussed. The IC_{50} values (24 h) of **1–4** for nasopharyngeal cancer cell line HK1 are in the range 2.2–5.2 μM while the corresponding values for normal cell line NP69 are greater than 13.0 μM. All complexes, at 5 μM, induced 41–60 % apoptotic cell death in HK1 cells but no significant cell death in NP69 cells.

Keywords Ternary copper(II) complexes · Crystal structure · DNA binding · G-quadruplex · Topoisomerase I · Anticancer selectivity

Introduction

Studying interactions of metal complexes with DNA and proteins have increased our understanding of cellular processes. Unlike metallosupramolecule, the small sizes of metal complexes seem to make them not suitable for DNA sequence-specific recognition because they cannot target more than 2–3 base pairs (Meistermann et al. 2002). Nevertheless, they do exhibit varying degree of binding selectivity. Cisplatin is an example of nucleobase selective covalent binding of metal complexes and the availability of two *cis*-labile ligands leads to inter- and intra-strand linkages involving only G-bases (Kostova 2006). Other metal complexes are known to bind preferentially to AT-sequences (Patra et al. 2007; Rajendiran et al. 2008; Eriksson et al. 1994; Franklin et al. 1996; Wheate and Collins 2000) or CG-sequences (Wheate and Collins 2000; Gao et al. 2008; Wu et al. 2005; Kikuta et al. 2000; Tan et al. 2010). Inhibition of restriction enzymes (RE), which binds to short specific nucleobase sequences and cleaves DNA strands at specific site(s), suggest binding of metal complexes at these specific sequences and thus having similar selective binding (Nakabayashi et al. 2006; Gallori et al. 2000; Snow and Sheardy 2001).

The mechanism of the above preferential binding to AT- and CG-sequences is not fully understood. Preferential binding of cationic metal complexes to AT-sequences than to CG-sequences was attributed to greater electrostatic interaction (Wheate and Collins 2000). It was mentioned that AT sequences have greater electrostatic potential than GC sequences in the minor groove. Chakravarty et al. found that copper(II) bis-arginate $[Cu(L\text{-arg})_2](NO_3)_2$ and [Cu(L-arg)(phen)Cl]Cl exhibited preferential binding to poly(dA)·poly(dT) than to poly(dG)·poly(dC) (Patra et al. 2007). It seems that the positively charged guanidiunium end groups of arginine is important in this recognition as these copper(II) complexes are structurally similar to netropsin, which also exhibit AT-binding preference. Other non-intercalating forces, involving van der Waals interaction and hydrogen bonding, are also involved in sequence selective binding. How relative contribution of these three types of interactive forces can lead to recognition selectivity is not clear. Geometric shape of the metal complexes may be a contributing factor as exemplified by both square planar $Pt(en)_2^{2+}$ (en = ethylenediamine) and Ni(II)-peptide complexes binding selectively to AT sequence of duplex oligonucleotides (Franklin et al. 1996). However, AT-selective binding by Δ- and Λ-$[Ru(phen)_3]^{2+}$ seems to be coincidental when they are located in the minor groove of the given DNA (Eriksson et al. 1994).

Barton and co-workers were able to design octahedral intercalating metal complexes to bind selectively to specific DNA sequences by making use of the small variation in the shape and functionalities of the DNA grooves (Erkkila et al. 1999; Zeglis et al. 2007). This was achieved by using large planar aromatic intercalating ligand to bind to DNA and ancillary ligands to achieve binding selectivity within the major groove. For example, Δ-$[Rh(DPB)_2(phi)]$ (DPB = 4,4-diphenylbipyridine; phi = 9,10-phenanthrenequinone diamine) readily bound at the sequence 5′-CTCTAGAG-3′ and inhibited the *Xba*I RE with the same recognition site (Sitlani et al. 1993; Sitlani and Barton 1994). The $[Rh(R,R\text{-})Me_2trien](phi)]^{3+}$ ((*R*,*R*)-Me_2trien = 2*R*, 9*R*-diamino-4,7-diazadecane) was found to be able to recognize 5′-TGCA-3′ via hydrogen bonding between the axial amines and the O6 of guanine, as well as by van der Waals contacts between the pendant methyl groups and the methyl groups of thymine (Krotz et al. 1993). Another approach was reported to involve conjugating a polynucleotide (DNA recognition domain) to the coordinated ligand of the metal complex (Chen and Sigman 1986; Francois et al. 1989; Mestre et al. 1997).

Unlike that involving DNA, interaction of metal complexes with topoisomerase is a relatively new field of research. Topoisomerases are produced when needed for certain biological processes involving DNA, and degraded by proteasome when not needed. They are important enzymes in the nucleus that modify the topological state of DNA by the introducing transient breaks in the DNA strands (Wang et al. 1998). Mitosis, particularly DNA transcription and replication, require topoisomerases. Recent development in cancer chemotherapy and antimicrobial agents has focussed on targeting the topoisomerase (Kumar Singh et al. 2007). Thus far, topoisomerase I (Topo I) inhibitors which are mainly organic compounds, have a wide range of antitumor activities and are among the most widely used anticancer drugs clinically (Sunami et al. 2009; Rothenberg 1997; Beretta et al. 2008; Teicher 2008; Pommier 2006). In fact, Topo I and II are now established as molecular targets of anticancer drugs and their inhibition induces cancer cell death by apoptosis (Arjmand and Muddassir 2010; Chashoo et al. 2011). Later, it was realised that these organic compounds also possess DNA sequence-selective activity as evidenced by stabilization of topoisomerase-DNA cleavage complexes at specific sites (Capranico et al. 1997; Arimondo et al. 2006; Rao et al. 2007). Two common features of Topo I poisons are that they are base-pairs intercalators and have hydrogen-bond acceptor on the minor groove binding site of the drugs (Gan et al. 2011). Such investigation, naturally, has also attracted inorganic chemists. Copper(II) chloride was found to inhibit Topo I, extracted from shrimp, at millimolar concentration (Chuang et al. 1996). Among a series of metal(II) pyrophosphate-bridged complexes, $\{[M(phen)_x]_2(\mu\text{-}P_2O_7)\}$ (where $x = 1$ or 2), the copper complex could inhibit Topo I at micromolar concentrations (Ikotun et al. 2009). A series of Cu(II)–M(II) bimetallic complexes (M(II) = Cu, Co, Ni, Mn, Zn) were also found to significantly inhibit Topo I in mutant yeast strains at 5 μM (Rupesh et al. 2006). Recently, new heterobimetallic complexes containing Cu(II)–Sn_2(IV)/Zn(II)–Sn_2(IV) cores and salicylaldimine pharmacophore were found to be DNA groove binders and could inhibit Topo I and II (Arjmand and Muddassir 2010).

G-quadruplex, a non-B form DNA structure, is also a new molecular target in the development of anticancer drugs (Miller and Rodriguez 2011; Neidle 2010). G-quadruplex DNA motifs, such as TTAGGG-repeats, occur at DNA telomeric ends and throughout the human genome. Over 350,000 predicted DNA sequences in the genome can fold into G-quadruplex structures. Not surprisingly, extensive research into interaction of small molecules with G-quadruplex has been reported. However, quadruplex stabilizers are mainly organic heteroaromatic compounds. Similar reports involving metal complexes are less numerous Xu et al. (2010).

Improving the efficacy and reducing toxic side-effects of metal-based drugs, such as cisplatin, have been the major concern of on-going anticancer research. Tan et al. reported the possible relationship between the DNA-binding selectivity of a neutral nickel(II)-quercetin complex and the down-regulation of survivin gene (which is selectively expressed in most tumor cells), and the link to its efficient induction of apoptosis in three tumor cell lines (Tan et al. 2010). Unfortunately, the nickel(II) complex was not tested on the corresponding normal cell lines. There seems to be no similar report of the relationship between the DNA-binding selectivity of metal complexes and their selective anticancer property on cancer cells over normal cells.

In southern China, Malaysia and other South East Asian countries, nasopharyngeal cancer (NPC) is the most common head and neck cancer (Sung et al. 2005). Current treatment with cisplatin, paclitaxel and radiotherapy or combination thereof has not been quite satisfactory for advanced and metastatic NPC. Even treatment of this cancer with a new generation, therapeutic monoclonal antibody drug directed against epidermal growth factor receptor elicited only positive response from 13 % of patients although the treatment was well tolerated with minimum adverse effect (Vermorken et al. 2007). Therefore, there is a need to explore new drugs which are more efficient and safe. As far as we know, copper complexes have not been investigated as anticancer drugs for NPC although copper is an essential micronutrient and its compound could be less toxic than compounds of platinum and other transition metals.

Herein, we present the effect of the position and the number of methyl substituent(s) in the auxiliary ligand, methylated glycine derivative, of the mixed-ligand copper(II) complexes with 1,10-phenanthroline (Fig. 1) on their crystal structure, their binding with G-quadruplex and DNA duplexes, their inhibition of RE and Topo I, and their differential cytotoxicity towards NPC (HK1) and normal (NP69) cells. X-ray crystallography, FTIR, CHN analysis, UV–visible,

conductivity measurement, ESI–MS, fluorescence spectroscopy, electron paramagnetic resonance (EPR) spectroscopy, CD spectroscopy, gel electrophoresis, MTT colorimetric assay and apoptosis study using flow cytometry were employed in this study.

Materials and methods

Materials

The amino acids (aa), viz. glycine (gly), L-alanine (L-ala), 2-methylalanine or 2,2-dimethylglycine (C-dmg) and sarcosine or *N*-methylglycine (sar), were purchased from Acros Organic (Fisher Scientific). Most of the chemicals and reagents were of analytical grade and were used as supplied. The pBR322, Lambda DNA (λ DNA), gene ruler 1 kb DNA ladder, ethidium bromide (EB), loading buffer, *Tris*-(hydroxymethyl) aminomethane (Tris), and agarose were bought from BioSyn Tech (Fermentas). The synthetic oligonucleotides (PAGE purified) were ordered from 1st Base Sdn Bhd (Malaysia) and were used as supplied. Calf thymus DNA (CT-DNA) was obtained from Sigma. All solutions for DNA experiments were prepared with ultra-pure water from an Elga PURELAB ULTRA Bioscience water purification system with UV light accessory. The Tris-HCl-NaCl buffer (TN) was prepared using the above water. This Tris-HCl buffer contained 50 mM NaCl and the pH of the buffer solution was adjusted to the required value by addition of concentrated hydrochloric acid or sodium hydroxide. All stock solutions of buffers were autoclaved at 121 °C. The nasopharyngeal cell lines, viz. cancer cell line HK1, and normal cell line NP69, were from George SW Tsao (Hong Kong University). All cell culture products were purchased from Invitrogen (Grand Island, NY). 3-[4,5-Dimethylthiazol-2-yl]-2,5-diphenyltetrazolium bromide (MTT) was purchased from Sigma-Aldrich (St. Louis, MO) while Annexin V-FITC Apoptosis Detection Kit II was purchased from BD Biosciences (MA, USA). A known anticancer compound, *bis*(8-hydroxyquinolato)copper(II), abbreviated as [Cu(8OHQ)$_2$], was purchased from Sigma-Aldrich.

Methods and instrumentation

Elemental analysis of C, N and H was carried out on a Perkin Elmer 2400 CHN analyzer. The FTIR spectra of the complex were recorded as KBr pellets in the range 4,000–400 cm^{-1} on a Perkin Elmer FT-IR spectrometer. Visible spectroscopic measurement was carried out on a Perkin-Elmer Lambda 40 spectrophotometer in the range 200–900 nm. A CON 700 bench top conductivity meter from EUTECH Instruments was used to measure the conductivity of the solvents and methanol–water (v/v 1:1) solutions of the copper(II) compounds. The positive-ion electrospray ionization–mass spectra (ESI–MS) of the four copper(II) complexes, dissolved in methanol, were obtained using Thermo Finnigan LCQ mass spectrometer (National University of Singapore). X-band EPR spectra (9.02–9.04 GHz) were measured on JEOL JES-RE2X spectrometers with 100 kHz field modulation of 0.5 mT. The fluorescence study was carried out with a Perkin-Elmer LS55 Fluorescence spectrometer. Fluorescence study of the interaction of copper(II) complexes with CT-DNA or ds(oligonucleotide) was carried out with a 1.0 cm quartz cell. Circular dichroism study of the interaction of copper(II) complexes with DNA was carried out with a 1.0 cm or 1.0 mm quartz cells respectively using a Jasco J-810 spectropolarimeter. For studies on aqueous solution samples, distilled water was filled into the reference cell while for studies in buffered solution the corresponding buffer was used as the reference.

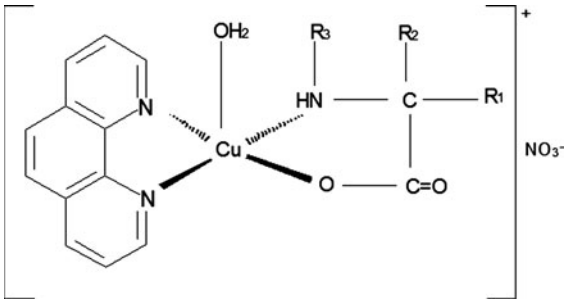

Fig. 1 Structure of [Cu(phen)(aa)(H$_2$O)]NO$_3$ (gly: R$_1$ = R$_2$ = R$_3$ = H; DL-ala: R$_1$ = CH$_3$; R$_2$ = R$_3$ = H; C-dmg: R$_1$ = R$_2$ = CH$_3$, R$_3$ = H; sar: R$_1$ = R$_2$ = H; R$_3$ = CH$_3$)

Synthesis of copper(II) complexes

The series of [Cu(phen)(aa)(H$_2$O)]NO$_3$·*x*H$_2$O complexes **1**–**4** (Fig. 1; aa: gly, **1**; DL-ala, **2**; C-dmg, **3**; sar, **4**. *x* = 0, 1½, 2½) were prepared. A typical example is given for the preparation of [Cu(phen)(DL-ala)(H$_2$O)]-NO$_3$·2½H$_2$O **2**. L-alanine (0.09 g, 0.001 mol) was

added to a water–ethanol mixture of $Cu(NO_3)_2{\cdot}3H_2O$ (0.25 g, 0.001 mol) and 1,10-phenanthroline (0.20 g, 0.001 mol) to give a dark blue solution. The solution was raised to pH 8.1 with NaOH solution. On heating the resultant solution in water-bath at 45 °C overnight, blue needle crystals were obtained. Yield: 0.18 g, 40 %. Repeated attempts yielded suitable crystal for X-ray crystal structure analysis.

[Cu(phen)(gly)(H_2O)]$NO_3{\cdot}1½H_2O$, **1**. Except for ESI–MS, this literature compound has been previously characterized (Zhang and Zhou 2008). Calculated *m/z* (ESI–MS) of $[Cu(phen)(gly)]^+$ species: 317.2 for ^{63}Cu (62.9296; relative abundance, 69.17) and 319.2 for ^{65}Cu (64.927792; relative abundance, 30.83).

[Cu(phen)(DL-ala)(H_2O)]$NO_3{\cdot}2½H_2O$, **2**. Calc. for $C_{15}H_{19}N_4O_{7.5}Cu$: C, 41.05; H, 4.36; N, 12.77 %. Found: C, 41.13; H, 4.25; N, 12.76 %. FTIR (cm^{-1}): ν_{OH}(water) 3468s; ν_{NH}(amino) 3230s; ν_{COO^-}(asym,-sym) 1636vs, 1384vs; ρ_{CH}(phen) 858s, 723s. Found: *m/z* (ESI–MS) 330.8 (100 %), 332.8 (~44 %). Calculated *m/z* of $[Cu(phen)(ala)]^+$ species: 331.2 for ^{63}Cu (62.9296; relative abundance, 69.17) and 333.2 for ^{65}Cu (64.927792; relative abundance, 30.83).

[Cu(phen)(C-dmg)(H_2O)]NO_3, **3**. Calc. for $C_{16}H_{18}N_4O_6Cu$: C, 45.12; H, 4.26; N, 13.16 %. Found: C, 45.43; H, 4.09; N, 13.24 %. FTIR (cm^{-1}): ν_{OH}(water) 3437s; ν_{NH}(amino) 3235s; ν_{COO^-}(asym,sym) 1663vs, 1384vs; ρ_{CH}(phen) 848s, 722s. Found: *m/z* (ESI–MS) 344.8 (100 %), 346.8 (~43 %). Calculated *m/z* for $[Cu(phen)(C\text{-}dmg)]^+$ species: 345.3 for ^{63}Cu (62.9296; relative abundance, 69.17) and 347.2 for ^{65}Cu (64.927792; relative abundance, 30.83).

[Cu(phen)(sar)(H_2O)]NO_3, **4**. Calc. for $C_{15}H_{16}N_4O_6Cu$: C, 43.74; H, 3.92; N, 13.60 %. Found: C, 43.69; H, 3.95; N, 13.49 %. FTIR (cm^{-1}): ν_{OH}(water) 3331s; ν_{NH}(amino) 3197s; ν_{COO^-}(asym,sym) 1655vs, 1384vs; ρ_{CH}(phen) 859s, 724s. Found: *m/z* (ESI–MS) 330.8 (100 %), 332.8 (~44 %). Calculated *m/z* of [Cu(phen)(sar)]$^+$ species: 331.2 for ^{63}Cu (62.9296; relative abundance, 69.17) and 333.2 for ^{65}Cu (64.927792; relative abundance, 30.83).

X-ray crystallography data for [Cu(phen)(aa)(H_2O)]$NO_3{\cdot}xH_2O$ (**2**, aa = DL-ala, $x = 2½$; **3**, aa = C-dmg, $x = 0$)

Intensity data for blue needle crystals of **2** (0.34 × 0.11 × 0.06 mm) and **3** (0.42 × 0.16 × 0.09 mm), were collected at 293 K on a Bruker SMART APEX area-detector and at 100 K on a Bruker APEXII Duo CCD area detector with both using MoKα radiation, $\lambda = 0.71073$ Å, over the range $2.44° < \theta < 26.37°$ and $2° < \theta < 26°$ respectively. SHELXS-97 and SHELXL-97 were used for solution and refinement of **2** (Sheldrick 1997a, b). Apex2 software and SHELXTL was used for data collection, solution and refinement of **3** (Bruker 2009; Sheldrick 2008). Absorption corrections for **2** and **3** were made using SADABS (Sheldrick 1996) and SADABS (Bruker 2009) respectively. The structure was solved by direct-methods and refined by a full-matrix least-squares procedure on F^2 with anisotropic displacement parameters for non-hydrogen atoms, C and N-bound hydrogen atoms in their calculated positions and a weighting scheme of the form calculated $w = 1/\left[s^2\left(F_o^2\right) + (0.0000P)^2 + 75.6448P\right]$ where $P = \left(F_o^2 + 2F_c^2\right)/3$ (for **2**) and $w = 1/\left[s^2\left(F_o^2\right) + (0.0244P)^2 + 0.6037P\right]$ where $P = \left(F_o^2 + 2F_c^2\right)/3$ (for **3**). Data collection and experimental details for the complex are summarized in Table 1 while the selected bond distances and angles are given in Table 2. The molecular structures of **2** and **3** are shown in Figs. 2 and 3. The structure **2** exhibited disorder of the alanine. This was modelled as disorder of the CH_3CH fragment over two sites of equal occupancies and corresponds to racemisation at C24; and appropriate restraints on the bond distances were employed. A hydrogen atom was not added to the molecular formula for one of the half water molecule as it was disordered. The formula of **2** is given as $CuC_{15}H_{18}N_4O_{7.5}$ with one hydrogen atom less. The crystallographic data for **2** and **3** have been deposited as CCDC 809125 and 809126 respectively. These data can be obtained free of charge via http://www.ccdc.cam.ac.uk/conts/retrieving.html, or Cambridge Crystallographic Data Centre, 12 Union Road, Cambridge CB2 1EZ, UK; fax: (+44) 1223-336-033; or e-mail: deposit@ccdc.cam.ac.uk.

DNA Binding studies

Stock solutions of CT-DNA were prepared by dissolving the DNA in buffer solution at 4 °C, and the resultant homogeneous solutions were used within 2 days. The concentration of CT-DNA per nucleotide phosphate was calculated from the absorbance at 260 nm by using $\varepsilon = 6600\ M^{-1}\ cm^{-1}$ (Reichmann et al. 1954). The purity of the DNA was checked by

monitoring the absorbance at 260 and 280 nm. PAGE grade self-complimentary 12-mer oligonucleotides $(CG)_6$, $(AT)_6$, HPLC grade G-quadruplex 22-mer oligonucleotide 5′-AGGGTTAGGGTTAGGGTTAGGG-3′, and 17-mer complementary oligonucleotides 5′-CCAGTTCGTAGTAACCC-3, 3′-GGTCAAGCATCATTGGG-5′ were annealed, to give the respective duplex and G-quadruplex, as specified by the suppliers, 1stBASE and Eurogentec Ait. The circular dichroism spectra were obtained by scanning TN (5 mM Tris; 50 mM NaCl, pH 7.5) buffered solutions of the DNA without and with complexes **1**–**4**. Fluorescence (FL) emission spectra in the study of EB quenching assay in finding the DNA apparent binding constants of complexes **1**–**4** were recorded in the wavelength range 550–650 nm by exciting the solutions respectively with light at 545 nm. Excitation and emission slits were set at 10 nm. Solutions of DNA, and the series of complexes **1**–**4** were prepared in TN buffer (5 mM Tris, 50 mM NaCl) at pH 7.5 unless specifically stated.

Binding constants from EB displacement assay

Binding constants of the copper(II) complexes **1**–**4** for various DNA duplexes were obtained through quantitative titration of the DNA saturated with bound EB with increasing concentration of copper(II) complexes. This is based on the competitive binding model reported in the literature (Borger et al. 2001). The competitive binding of the copper(II) complex to the DNA reduces the emission intensity of EB either by quenching its emission or displacement to its free state. Fluorescence measurements were obtained by using a Perkin-Elmer LS55 photoluminescence spectrometer at room temperature (RT). The excitation wavelength, λ_{ex} was set at 545 nm and the emission wavelength, λ_{em} was set at 600 nm at RT. For determination of binding constant of each copper(II) complex with CT-DNA, a TN buffer (5 mM Tris, 50 mM NaCl) at pH 7.5 was used. Prior to titration with the copper(II) complex, portions of 3 mL mixtures of EB (0.32 μM) and CT-DNA (10 μM) were incubated for 24 h to allow saturation of DNA with EB (Seng et al. 2009). The previously reported optimized conditions developed for a high-throughput method of determining binding constants of various compounds for a large collection of DNA hair-pin deoxyoligonucleotides of short nucleotide sequences were used in determining the binding constants of complexes **1**–**4** with duplex deoxyoligonucleotides (duplex oligo) (Borger et al. 2001). Similarly the ratio of duplex:EB is 1:2 and the TN buffer (pH 7.5) composition is 100 mM Tris and 100 mM NaCl. Prior to titration with copper(II) complex, portions of 3 mL mixtures of EB (2 μM) and duplex oligo (1 μM) were incubated for 24 h to attain saturation. For both cases, i.e. CT-DNA and duplex, the serial titration was completed by adding 1 μL of increasing concentration of copper(II) complex from appropriate stock solutions to the series of 3 mL EB–DNA mixtures until the quenching of DNA-bound EB fluorescence exceeded 50 %. The final reaction mixtures were incubated for 2 h before measurement of their fluorescence intensity. The fluorescence emission intensities were plotted against the complex concentration to yield a curve that showed the relative extent of quenching of DNA-bound EB. The values of the apparent binding constant, K_{app}, of the copper(II) complexes were calculated from the equation $K_{app,[complex]}[complex] = K_{app,EB}[EB]$ where $K_{app,EB}$ is the apparent binding constant of EB (which is usually assigned as $10^7\ M^{-1}$), $K_{app,complex}$ is the apparent binding constant of copper(II) complex, [EB] is the concentration of EB used and [complex] is the concentration of the copper(II) complex at 50 % quenching (Borger et al. 2001; Rajendran and Nair 2006).

RE inhibition assay

The RE inhibitory activity was determined by observing the resultant band of λ DNA. Each reaction mixture contained 0.25 μg of λ DNA, 2 μL of 10× RE reaction buffer, 50 μM of copper(II) complex, 5 units of RE and sterile deionized water. The total volume of each reaction was 20 μL. Firstly, λ DNA was incubated with copper(II) complex at 37 °C for 60 min and RE added before the reaction mixture was incubated for another 2 h at the same temperature. The reactions were terminated by the addition of 2 μL of 10 % sodium dodecyl sulphate (SDS), and then followed by 3 μL of dye solution comprising 0.02 % bromophenol blue and 50 % glycerol. The mixtures were applied to a 2.0 % agarose gel and electrophoresed for 2 h at 80 V with running buffer of Tris-acetate EDTA (TAE). The gel was stained, destained, and photographed under UV light using a Syngene Bio

Table 1 Crystal data and structure refinement of complexes **2** and **3**

	2	**3**
	[Cu(phen)(DL-ala)(H$_2$O)]·2½H$_2$O	[Cu(phen)(C-dmg)(H$_2$O)]
Formula	$C_{15}H_{18}N_4O_{7.5}Cu$	$C_{16}H_{18}N_4O_6Cu$
Formula weight	437.87	425.88
Crystal system	Monoclinic	Triclinic
a (Å)	20.2419(4)	7.3113(12)
b (Å)	6.98050(10)	11.4021(7)
c (Å)	25.1351(5)	12.0234(7)
α (°)	90.00	117.917(1)
β (°)	97.2985(10)	102.920(2)
γ (°)	90.00	93.039(2)
V (Å^3)	3522.78(11)	848.66(16)
Space group	$C2/c$	$p\bar{1}$
Z	2	2
ρ_{calc} (g cm^{-3})	1.651	1.667
$F(000)$	1800	438
Index ranges	$-25 \le h \le 25$; $-8 \le k \le 8$; $-30 \le l \le 31$	$-9 \le h \le 9$; $-14 \le k \le 12$; $-14 \le l \le 14$
Final R indices [$I > 2\sigma(I)$]	$R_1 = 0.0785$, $wR_2 = 0.1812$	$R_1 = 0.0208$, $wR_2 = 0.0549$
R indices (all data)	$R_1 = 0.0846$, $wR_2 = 0.1832$	$R_1 = 0.0219$, $wR_2 = 0.0558$
θ Range (°)	2.44–26.37	2.0–26.0
Reflections	18,749	3,259
Independent reflections	3,610 [R(int) = 0.0449]	3,121 [R(int) = 0.0188]
Goodness-of-fit on F^2	1.362	1.066
Residuals (e Å^{-3})	0.853, −0.729	0.328, −0.304

Imaging system and the digital image viewed with Gene Flash software.

Binding constants from thiazole orange quenching assay

Thiozole orange (TO) quenching studies were conducted using oligo 5′-AG$_3$(T$_2$AG$_3$)$_3$-3′ (22-G), and two complementary 17 nucleotide primers (17 bp), 5′-CCAGTTCGTAGTAACCC-3′ and 3′-GGTCAA GCATCATTGGG-5′ as previously reported (Seng et al. 2009). Previous researchers have shown that 22-G folds into a G-quadruplex while 17 bp adopts a duplex DNA structure. Binding to each oligonucleotide was determined by titrating the copper(II) complex into a solution containing the oligonucleotide (1 μM) and TO (2 μM) in 10 mM cacodylate buffer (pH 7.2) supplemented with 100 mM NaCl. Each fluorescence spectrum was recorded and the area under the peak was determined using the instrument software for every addition of the copper(II) complex. The area was plotted as a function of copper(II) complex concentration and the concentration of copper(II) complex that reduced the area under the peak by 50 % was taken as the QC_{50} value. Binding constants were calculated assuming a simple competitive binding model (Stern–Volmer equation). The values of the apparent binding constant, K_{app}, of the metal complex were calculated from the equation $K_{app,[complex]}[complex] = K_{app,TO}[TO]$ where $K_{app,TO}$ is the apparent binding constant of TO with a literature value of 3×10^6 M^{-1} (Monchaud et al. 2008), $K_{app,complex}$ is the apparent binding constant of copper(II) complex, [TO] is the concentration of TO used and [complex] is the concentration of the copper(II) complex at 50 % quenching (i.e. QC_{50}).

DNA-fiber EPR

Preparation of DNA-fibers containing paramagnetic copper(II) complexes, instrumentation and EPR measurements were carried out as described previously. The DNA from salmon testes was dissolved in 20 mM NaCl to make a solution of approximately 1 mM DNA base pair concentration. Subsequently, the complex solution was added drop wise to the DNA, and stirred for approximately 12 h at 4 °C. The DNA-pellet was obtained by ultracentrifugation of the mixed solution at 60000 rpm for 7 h. The DNA fibers were prepared from the pellet as previously reported (Chikira et al. 1997; Chikira 2008).

Topo I assay

The human DNA Topo I inhibitory activity by copper(II) complexes **1–4** was determined by measuring the relaxation of supercoiled plasmid DNA pBR322. Each reaction mixture contained 10 mM Tris–HCl, at pH 7.5, 100 mM NaCl, 1 mM phenylmethylsulfonyl fluoride (PMSF), and 1 mM 2-mercaptoethanol, 0.25 μg plasmid DNA pBR322, 1 unit of human DNA topo I, and the copper(II) complex at a specified concentration. Total volume of each reaction

Table 2 Selected bond lengths (Å) and angles (°) of complexes **1–3**

1			**2**			**3**		
Cu1–N1	2.000(6)	phen	Cu1–N1	2.010(5)	phen	Cu1–N1	2.0018(13)	phen
Cu1–N2	1.997(6)	phen	Cu1–N10	2.013(5)	phen	Cu1–N2	2.0246(13)	phen
Cu1–N3	1.984(6)	gly	Cu1–N25	1.988(6)	ala	Cu1–N3	1.9763(13)	C-dmg
Cu1–O2	1.920(5)	gly	Cu1–O21	1.949(4)	ala	Cu1–O1	1.9429(10)	C-dmg
Cu1–O1W	2.280(7)	water	Cu1–O1W	2.270(5)	water	Cu1–O1W	2.3688(12)	water
N1–Cu1–N2	82.9(2)	phen	N1–Cu1–N10	82.6(2)	phen	N1–Cu1–N2	82.28(5)	phen
N3–Cu1–O2	83.8(2)	gly	N25–Cu1–O21	84.5(2)	ala	N3–Cu1–O1	85.11(5)	C-dmg
N1–Cu1–N3	98.3(2)		N10–Cu1–N25	98.1(2)		N2–Cu1–N3	97.12(5)	
N2–Cu1–O2	93.4(2)		N1–Cu1–O21	93.1(2)		N1–Cu1–O1	95.50(5)	
N2–Cu1–N3	163.5(3)		N1–Cu1–N25	169.0(3)		N1–Cu1–N3	172.82(5)	
N1–Cu1–O2	173.7(3)		N10–Cu1–O21	170.4(2)		N2–Cu1–O1	177.77(5)	
N1–Cu1–O1W	92.1(3)		N1–Cu1–O1W	90.7(2)		N1–Cu1–O1W	90.30(5)	
N2–Cu1–O1W	97.7(3)		N10–Cu1–O1W	94.7(2)		N2–Cu1–O1W	89.47(5)	
N3–Cu1–O1W	98.8(3)		N25–Cu1–O1W	100.1(2)		N3–Cu1–O1W	96.85(5)	
O2–Cu1–O1W	93.4(3)		O21–Cu1–O1W	93.96(18)		O1–Cu1–O1W	90.31(4)	

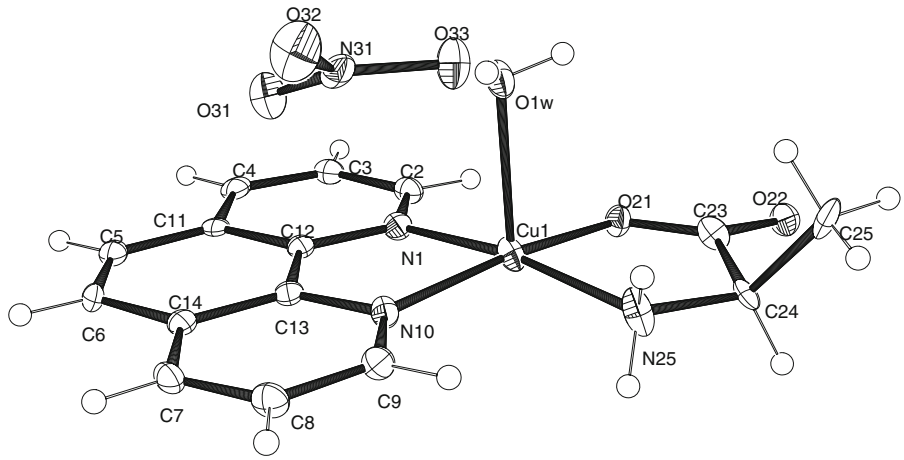

Fig. 2 Ortep plot of [Cu(phen)(DL-ala)(H_2O)] $NO_3 \cdot 2½H_2O$, **2**, showing one molecule with one of the coordinated alanine isomer (The lattice water molecules are not shown for clarity)

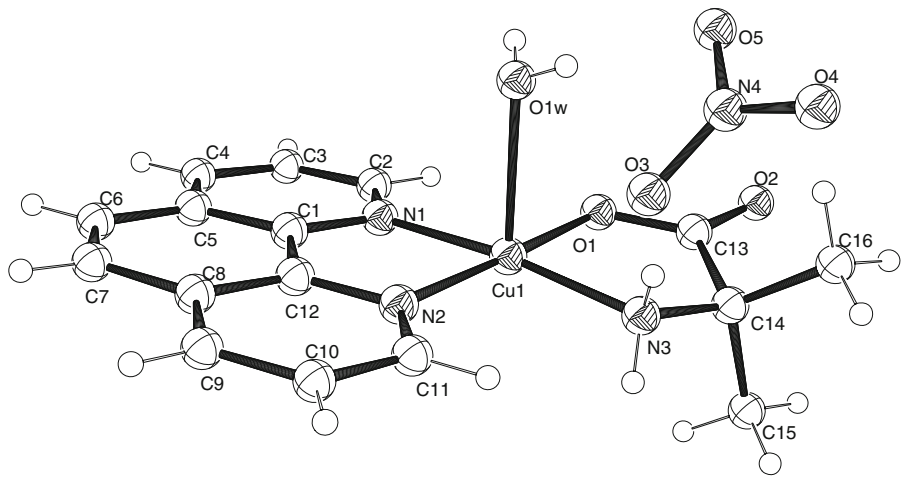

Fig. 3 Ortep plot of [Cu(phen)(C-dmg)(H_2O)]NO_3, **3**

mixture was 20 μL and these mixtures were prepared on ice. Upon enzyme addition, reaction mixtures were incubated at 37 °C for 30 min. Each reaction was terminated by the addition of 2 μL of 10 % SDS, and then followed by 3 μL of dye solution comprising 0.02 % bromophenol blue and 50 % glycerol. The mixtures were applied to a 1.2 % agarose gel and electrophoresed for 5 h at 33 V with running TAE buffer. The gel was stained, destained, and photographed under UV light using a Syngene Bio Imaging system and the digital image viewed with Gene Flash software.

The effect of sequential mixing of topo I, plasmid DNA pBR322 and copper(II) complex in the above topo I inhibition assay was also investigated for all the complexes, **1**–**4**. Three different sequential mixings were used. In the first case, human DNA topo I incubated with copper(II) complexes at 37 °C for 30 min before DNA was added and the reaction mixture was incubated for another 30 min at the same temperature. In the second case, copper(II) complex and DNA were incubated for 30 min at 37 °C first before the addition of human DNA topo I and a further incubation of 30 min at same temperature. In the third case, all three components were mixed simultaneously and incubated for 30 min at 37 °C.

Anticancer studies

Culture of nasopharyngeal cell lines

HK1 (a kind gift from Professor George SW Tsao, Hong Kong University, Hong Kong), an Epstein–Barr virus (EBV) negative nasopharyngeal carcinoma cell

line, was derived from a patient from Hong Kong. HK1 cells, was maintained at 37 °C in a humidified atmosphere of 5 % CO_2 in RPMI 1640 medium (Gibco, Invitrogen, CA, USA) supplemented with 10 % fetal bovine serum (FBS) (Gibco, Invitrogen, CA, USA), 50 U/mL penicillin (Invitrogen, CA, USA) and 50 μg/mL streptomycin (Invitrogen, CA, USA). The identity of HK1 cells was validated by DNA fingerprinting using AmpFISTR Identifiler® PCR amplification kit (Applied Biosystems, USA) and confirmed mycoplasma free by regular testing using VenorGeM® mycoplasma detection kit (Minerva biolabs, Germany). NP69-SV40T (NP69) (also a kind gift from George SW Tsao), an immortalised nasopharyngeal epithelial cell line was maintained in keratinocyte-serum free media (KSFM) supplemented with 25 μg/mL bovine pituitary extract (BPE) and 0.16 ng/mL recombinant epidermal growth factor (Gibco, USA), 50 U/mL penicillin and 50 μg/mL streptomycin.

MTT viability assay

HK1 and NP69 were harvested from exponential growth phase maintenance cultures. Cells were seeded at a density 1×10^5 cells/mL in 100 μL medium per well in a 96-well flat bottom tissue culture plate (Orange Scientific), followed by incubation at 37 °C in a 5 % CO_2 incubator overnight to allow the cells to attach to the wells. The cells were washed using phosphate buffer solution (PBS) and the culture media replaced with 100 μL of fresh culture media with or without test compounds before being incubated for a further 24 h under the same conditions. Cells were treated with six different compound concentrations (25, 12.5, 6.25, 3.12 and 1.56 μM) of complexes **1**–**4** and $Cu(8OHQ)_2$. Each set of experiment was done in triplicate.

After 24-h incubation of cells with or without test compounds, a 20-μL solution of MTT in PBS (5 mg/mL) was added to each well. The cells were incubated for a further 4 h under the same conditions to allow MTT to be metabolized. The plate was centrifuged at 1,000 rpm for 5 min. The viable cells producing formazan were inspected microscopically and the media were slowly aspirated. Then, 100 μL dimethyl sulfoxide (DMSO) per well was added to dissolve the formazan using a multichannel pipette. The optical density was measured using enzyme-linked immunosorbent assay (ELISA) plate reader (Dynatech MRX) at a wavelength of 570 nm with background subtraction at 630 nm. Every experiment included a set of negative controls (untreated cultures), and blank wells without cells. Percentage of cell viability was calculated using Microsoft Excel and IC_{50} values (the concentration of the complex causing 50 % growth inhibition) were estimated from dose response curves.

Calculation

$$\text{cell viability } (\%) = \frac{\text{Mean optical density of sample}}{\text{Mean optical density of control}} \times 100$$

Annexin V-FITC/PI double staining in flow cytometric analysis of apoptosis

Both HK1 and NP69 cells were cultured in separate 60 mm petri dishes for the apoptosis assay. When the cells reached 70–80 % confluency, they were treated separately with 5 μM complexes **1**–**4** and $Cu(8OHQ)_2$ for 24 h. Cells were also cultured without treatment as negative control. Apoptosis assay was performed using Annexin V-FITC Apoptosis Detection Kit II (BD Pharmingen™).

Suspension cells and adherent cells in each of the above samples were treated as described herein. The suspension cells in the culture medium were collected, washed with PBS and then collected. Adherent cells remaining in the petri dish were trypsinised with 1 mL accutase (Millipore) at 37 °C for 5 min to completely detach the cells. Both fractions of cells, i.e. collected suspension cells and detached adherent cells, were combined and centrifuged at 1,000 rpm for 5 min. The resultant pellet of cells was resuspended in 1× binding buffer and cell count performed. A solution with a cell population of 1×10^6 cells/mL was prepared and 100 μL of this solution containing 1×10^5 cells was transferred into a 12 × 75-mm, 5 mL polystyrene round bottom test tube (Becton, Dickson and company). FITC Annexin V (5 μL) and PI (5 μL) was added to each test tube. Cells were mixed gently and incubated for 15 min at RT in the dark before adding 400 μL of 1× binding buffer. All treated cells samples were filtered into labeled 12 × 75-mm, 5 mL polystyrene round bottom test tubes with cell strainer caps and analyzed immediately by fluorescent activated cell sorter (FACS Calibur, Becton–Dickinson).

Unstained cells, cells stained with Annexin V-FITC only and cells stained with PI only were used as

controls to set up compensation and quadrants. BD CellQuest Pro software was used to analyze the data.

Statistical analysis

Statistical analyses were performed on the apoptosis data using SAS 9.2 statistical software for Windows. Wilcoxon Rank Sum test (one-sided and two-sided) was performed to check for significance. A calculated value of $p < 0.05$ was considered statistically significant.

Results and discussion

Structures of complexes 1–4

Four complexes of the general formula [Cu(phen)(aa)(H_2O)]NO_3·xH_2O, **1–4** (amino acid (aa): gly, **1**; DL-ala, **2**; C-dmg, **3**; sar, **4**; x = number of water molecules), were synthesized and characterized. Their structures were confirmed by X-ray crystallography analysis of **2** and **3**. The molecular structures of **2** and **3** are shown in Figs. 2 and 3 respectively. Each molecule consists of a discrete distorted square pyramidal $[Cu(phen)(aa)(H_2O)]^+$ complex cation and a NO_3^- counter anion. For both cationic complexes, two nitrogen atoms of 1,10-phenanthroline, a carboxylate oxygen and an amino nitrogen atoms of the amino acid (DL-ala for **2**; C-dmg for **3**) form the basal plane of the pyramid. A weakly coordinated water molecule occupies the apical position. Complex **2** is racemic, i.e. exists as [Cu(phen)(DL-ala)(H_2O)]NO_3·2½H_2O, and has 2½ lattice water molecules. The original L-ala used to make **2** has racemised under basic condition used. There is no lattice water in **3**. These structures are similar to [Cu(phen)(gly)(H_2O)]NO_3·1½H_2O, **1** reported by Zhang and Zhou (2008). There seems to be no significant effect of the methyl substituent(s) on the structure of the $[Cu(phen)(aa)(H_2O)]^+$ in **1**, **2** and **3** except that **3** is least distorted. Since the FTIR of **4** is very similar to those of **1–3**, it was deduced that complex **4** may have the same structure as **1–3**.

Solution studies of complexes 1–4

The crystal structures of **1**, **2** and **3** show that each solid compound is ionic with NO_3^- as counterion. To study the species in solution and the lability of the coordinated amino acid, the molar conductivity of copper compounds **1–4**, $Cu(NO_3)_2$ and the aa ligands (i.e. where aa = gly, DL-ala, C-dmg respectively) in water–methanol were determined (Table 3). The poor conductivity of phen, L-ala, gly, sar and C-dmg ligands (0.85–1.42 Ω^{-1} cm^2 mol^{-1}) shows that they are non-electrolyte in water–methanol. $Cu(NO_3)_2$ has a molar conductivity of 143.35 Ω^{-1} cm^2 mol^{-1} typical of 2:1 electrolyte (Ikotun et al. 2009). Complexes **1–4** have molar conductivity values (51–58 Ω^{-1} cm^2 mol^{-1}) within the range of 1:1 electrolytes (Bolos et al. 1996), confirming the presence of uncoordinated NO_3^- as counterion. As their molar conductivity values were almost constant over 24 h, complexes **1–4** should remain as 1:1 electrolytes and should be cationic species, $[Cu(phen)(aa)(H_2O)]^+$, were probably stable in aqueous solution during this period. The visible region λ_{max} of the aqueous solutions of complexes **1–4** lies in the range 612–620 nm while that of aqueous solution of $Cu(NO_3)_2$ is about 800 nm (Table 4; Supplementary data: Fig. S1 show visible spectrum of **3**). There was no significant change in λ_{max} of each of the solutions of complexes **1–4** over 24 h, indicating no change in the coordination sphere of the copper(II) in each complex species in solution. Substitution of coordinated amino acid ligand with water molecule would shift the λ_{max} to longer wavelength. This is consistent with the above molar conductivity data analysis. In addition, the copper(II) cationic complex species dissolved in methanol were detected by ESI–MS. Each positive-ion ESI mass spectrum shows only two intense $[Cu(phen)(aa)]^+$ m/z peaks due to different isotopic copper (^{63}Cu and ^{65}Cu) with the correct isotopic distribution. There was no dissociation of phen and aa^- ligands (Supplementary data: Figs. S2.1–2.4). The coordinated water molecule in $[Cu(phen)(aa)(H_2O)]^+$ dissociates under the ESI–MS conditions, as observed in ESI–MS of other copper(II) complexes (Halder and Zangrando 2010; Ruíz et al. 2007).

Comparative EPR study of complexes 1–4 with salmon sperm DNA

The $g_{//}$ signals of all the complexes **1–4** became most intense at $\Phi = 0°$ and least at $\Phi = 90°$, indicating that they bind to DNA with the $g_{//}$ axis parallel to the DNA fiber axis. Such Φ dependence corresponds to the case when the copper coordination plane involving the phenanthroline moiety is parallel to the DNA base-pair, characterizing the intercalative or partially

Table 3 Molar conductivity (Ω^{-1} cm^2 mol^{-1}) of complexes **1–4** and other compounds at 1×10^{-3}M

Compounds	Time		
	0 h	1 h	24 h
1	53.10	53.37	55.92
2	51.77	52.13	54.61
3	56.13	56.53	58.05
4	56.65	56.78	58.05
$Cu(NO_3)_2$	143.35	143.18	143.72
Phen	1.21	1.33	1.61
L-ala	0.85	0.92	1.12
Sar	1.12	1.28	1.59
Gly	1.03	1.11	1.37
C-dmg	1.42	1.51	1.87
KCl[a]	1,413	1,412	1,402

[a] Supplied by instrument manufacturer as calibrant solution with unknown concentration

Table 4 Visible spectral data of 1×10^{-3}M $Cu(NO_3)_2$ and complexes **1–4** in water–methanol (1:1 v/v)

Compound	λ_{max} (molar absorbtivity)		
	0 h λ_{max}/nm (ε/M^{-1} cm^{-1})	1 h λ_{max}/nm (ε/M^{-1} cm^{-1})	24 h λ_{max}/nm (ε/M^{-1} cm^{-1})
$Cu(NO_3)_2$	799.50 (12.0)	803.03 (12.1)	839.14 (14.4)
1	615.99 (48.4)	618.89 (52.1)	620.92 (47.8)
2	615.56 (44.4)	611.98 (52.4)	615.73 (63.2)
3	612.03 (59.9)	608.92 (84.1)	610.50 (79.0)
4	619.96 (60.7)	620.00 (62.5)	624.04 (61.0)

intercalative binding mode of the complexes (Fig. 4; Supplementary Figs. S2.1–2.4). Similar EPR spectra have been reported for [Cu(phen)(aa)] complexes, where aa = glycine, leucine, serine, threonine, cysteine, methionine, asparagines, lysine, arginine and glutamine (Chikira et al. 2002). Two kinds of $g_{//}$ signals were observed clearly for **2**, **3**, $Cu(phen)Cl_2$, and weakly for **4** and **1**. The two $g_{//}$ values ($g_{1//} = 2.30$ and $g_{2//} = 2.23$) of $Cu(phen)Cl_2$ in frozen solutions have been assigned to $[Cu(phen)(OH_2)_2]^{2+}$ and $[Cu(phen)(OH_2)(OH)]^{+}$, respectively (Fig. 4) (Chikira et al. 2002). These results indicate that the amino acid residues of **2** and **3** partly dissociated upon binding to DNA. Interestingly, both complexes **2** and **3** have methyl substituent(s) at the α-carbon of the coordinated amino acid while complex **4** has a methyl substituent at the amino N-atom of its coordinated amino acid. Thus, the ease with which the coordinated α-amino acid in complexes **1–4** dissociates from the copper(II) upon binding to the DNA depends on the position of the methyl substituent(s). Upon binding to DNA, complexes **1–3** underwent dissociation easily with resultant loss of amino acid moiety whereas **4** showed prolonged dissociation. It should be noted that the EPR spectrum of a previously synthesized [Cu(phen)(mal)Cl] complex (Tan et al. 2008) (mal = maltolate) did not show any $g_{//}$ signal of the dissociated species, viz. $[Cu(phen)(OH_2)_2]^{2+}$ and $[Cu(phen)(OH_2)(OH)]^{+}$. This suggests that [Cu(phen)(mal)Cl] is more stable than complexes **1–4** and that it can intercalate to DNA without dissociation of mal moiety.

DNA binding studies with different B-form duplexes

The earlier section on solution studies showed that **1–4** are cationic species in solution. EPR, spectroscopic and viscosity data have shown that $[Cu(phen)(gly)(H_2O)]^{+}$ bind to duplex DNA by intercalation (Zhang and Zhou 2008; Chikira et al. 2002). EPR evidence in the previous section also showed that all the $[Cu(phen)(aa)(H_2O)]^{+}$ complexes with methylated glycine ligands bind to the DNA by intercalation. The methyl substituent(s) seems not to affect the mode of binding. By using EB displacement assay, we evaluated the apparent binding constants of the copper(II) complexes **1–4** for various DNA duplexes. This was to investigate any possible effect of the number and position of the methyl substituent of the methylated glycine ligand on the DNA binding affinity and selectivity of $[Cu(phen)(aa)(H_2O)]^{+}$. The binding constants of complexes **1–4** on CT-DNA, calculated based on the competitive binding model, are $1.20 \pm 0.15 \times 10^4$, $1.02 \pm 0.18 \times 10^4$, $1.09 \pm 0.22 \times 10^4$ and $5.30 \pm 0.13 \times 10^3$ respectively. These binding constants are higher than that for $Cu(phen)Cl_2$ which was found to be $4.00 \pm 0.04 \times 10^3$ (Seng 2010). The binding constant of **4** is lower than that of **1** (by 2×) whereas those of **2** and **3** are not significantly higher than that of **1**. The sar ligand in **1** has a methyl group at the amino nitrogen of the aa ligand whereas aa ligand in **2** and **3** have methyl group(s) at the corresponding α-carbon. It seems that the binding

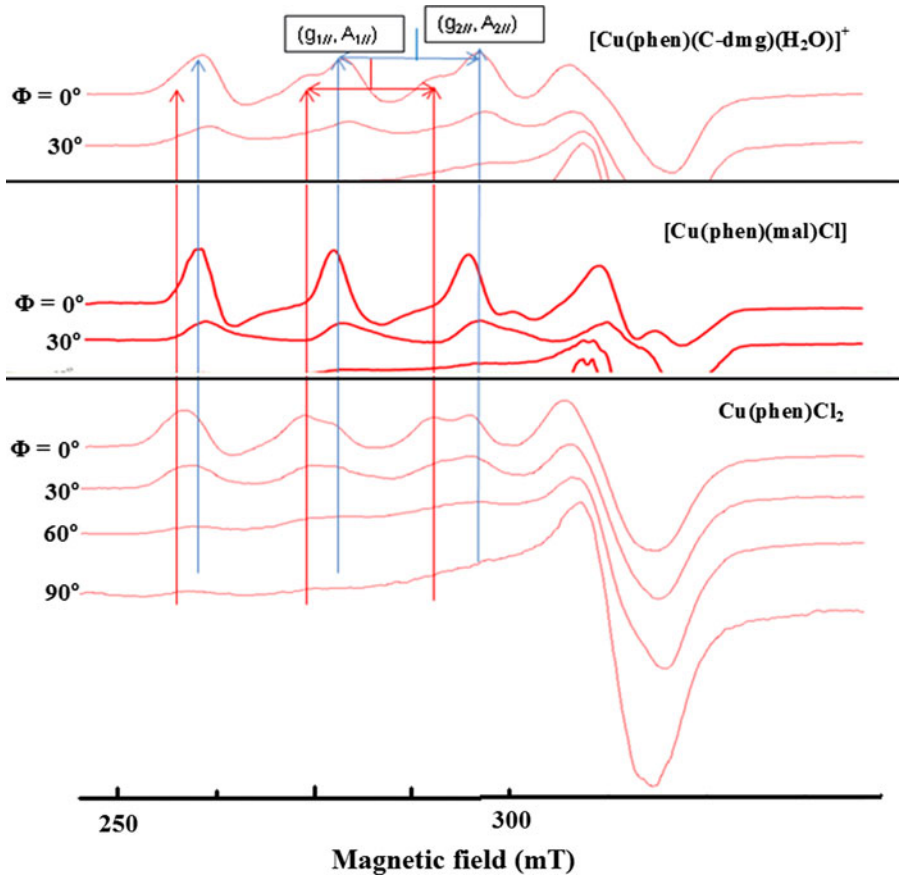

Fig. 4 EPR spectra of **3**, [Cu(phen)(mal)Cl] and [Cu(phen)Cl_2] on B-form DNA fibers at RT. Φ is the angle between the DNA-fiber axis and static magnetic field

affinity of $[Cu(phen)(aa)(H_2O)]^+$ for CT-DNA is only affected by the position of the methyl group at the amino nitrogen atom of the aa ligand.

The binding affinity of $[Cu(phen)(aa)(H_2O)]^+$ for $ds(AT)_6$ or $ds(CG)_6$ is not greatly affected by the number or position of the methyl substituent(s) of the amino acid moiety (Fig. 5a; Table 5). The presence of methyl substituent(s) in the methylated glycine in complexes **2**–**4** slightly enhanced the binding preference for CG or AT sequences in comparison to $[Cu(phen)(gly)(H_2O)]^+$ in (**1**)]. The presence of *N*-methyl group in complex **4** seems to have contrasting effect on the DNA binding constant. It significantly lowered the binding affinity of **4** for CT-DNA compared to **1** whereas it increased the binding affinity for both $ds(AT)_6$ and $ds(CG)_6$ duplexes. However, the binding constants of complexes **1**–**4** for the $ds(CG)_6$ is about twice those of the corresponding values for $ds(AT)_6$, suggesting greater selectivity of these complexes for CG sequences than AT sequences. Previously, it was found that cationic metal complexes prefer to bind to AT sequences than to CG sequences because of greater electrostatic interaction (Wheate and Collins 2000). The reason for this deviation is still unknown.

RE inhibition

To investigate the binding specificity of complexes **1**–**4**, a RE inhibition assay was used. Binding specificity of a metal complex can arise from the complex binding at the unique binding site of a RE which prevents the RE from binding at such sites on the λ DNA. As a result, the RE cannot cut the DNA. Consequently, a complex which can inhibit an RE is said to be binding selectively. A complex which inhibits less number of REs is said to bind more selectively as it binds to lesser number of such unique binding sites. Twelve RE (with binding site given in parentheses; ↓ denotes cutting site), viz. *Tsp* 5091 (5′-↓AATT-3′), *Mun*I (5′-C↓AATTG-3′), *Bst* 11071 (5′-GTA↓TAC-3′), *Nde*I (5′-CA↓TATG-3′), *Eco*RI

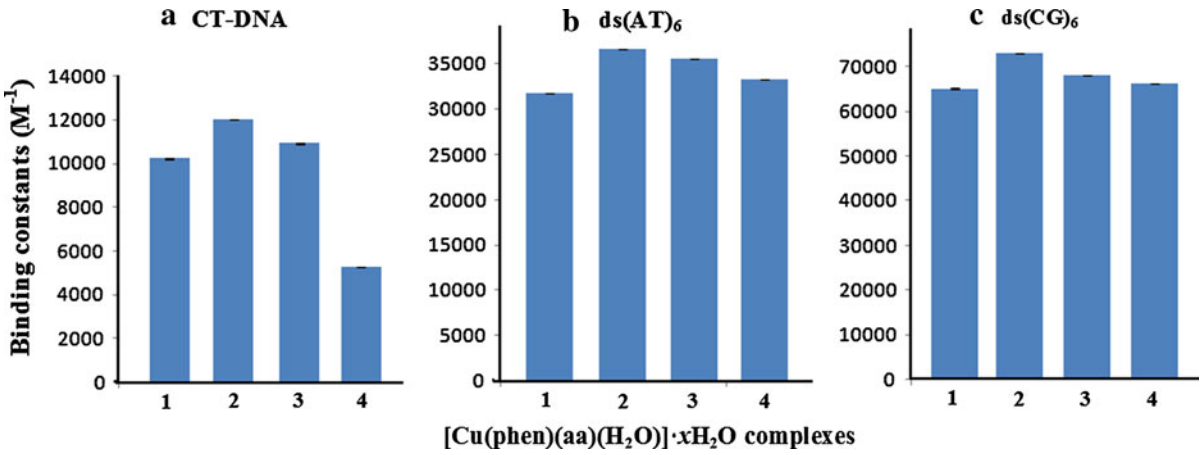

Fig. 5 Apparent binding constants (mean of triplicates) of complexes **1**–**4** for CT-DNA (**a**), ds(AT)$_6$ (**b**) and ds(CG)$_6$ (**c**) with standard deviations

Table 5 EB quenching assay results for complexes **1**–**4** on ds(AT)$_6$ and ds(CG)$_6$ oligonucleotides

Complex	Apparent binding constant (K_{app}) M^{-1} on ds(AT)$_6$	Apparent binding constant (K_{app}) M^{-1} on ds(CG)$_6$	K_{AT}/K^{a}_{CG}
1	$3.17 \pm 0.20 \times 10^4$	$6.51 \pm 0.14 \times 10^4$	0.49
2	$3.66 \pm 0.09 \times 10^4$	$7.31 \pm 0.18 \times 10^4$	0.50
3	$3.56 \pm 0.17 \times 10^4$	$6.81 \pm 0.13 \times 10^4$	0.52
4	$3.33 \pm 0.12 \times 10^4$	$6.62 \pm 0.10 \times 10^4$	0.50
Cu(phen)Cl$_2$	$3.17 \pm 0.09 \times 10^4$	$6.58 \pm 0.17 \times 10^4$	0.48

[a] K_{AT}/K_{CG} = ratio of K_{app}, ds(AT)$_6$/K_{app}, ds(CG)$_6$

(5′-G↓AATTC-3′), *Ase*I (5′-AT↓TAAT-3′), *Sca*I (5′-AGT↓ACT-3′), *Pvu*II (5′-CAG↓CTG-3′), *Sal*I (5′-G↓TCGAC-3′), *Pst*I (5′-CTGCA↓G-3′), *Hae*III (5′-GG↓CC-3′), and *Ssp*I (5′-AAT↓ATT-3′), were used. It was found that **1**, **2** and **4** inhibited *Ssp*I, *Ase*I, *Nde*I and *Bst* 11071 while **3** inhibited only *Ssp*I and *Nde*I (Supplementary data: Figs. S4.1–S4.4). The presence of only one methyl substituent in the methylated glycine moiety of **2** and **4** did not change the REs that can be inhibited, in comparison with REs inhibited by **1**. The copper(II) complexes **2** and **4** have the same binding selectivity as **1** which has unmethylated glycine. The binding selectivity of **3** is higher than those of **1**, **2** and **4** as the former inhibited lesser number of REs. The higher binding selectivity of complex **3** may be attributed to the presence of two α-methyl substituents. Interestingly, $CuCl_2$ and phen did not inhibit any of the 12 REs (data not shown) even though the respective complex Cu(phen)Cl$_2$ seems to bind, albeit selectively than **1**–**4**, as it inhibited 7 REs, viz. *Tsp* 509I, *Ase*I, *Ssp*I, *Mun*I, *Eco*RI, *Nde*I, and *Bst* 11071, under the same conditions (data not shown). This means that coordination of amino acid to the copper(II)-phen increases its DNA binding selectivity.

The effect of buffer ionic concentration (NaCl) on the DNA binding affinity of **1**–**4** was also studied. As expected, the binding constant of each copper complex decreased with increasing NaCl concentration (supplementary data, Table S1; 0–40 mM) and this corroborated our findings that **1**–**4** exists as cationic $[Cu(phen)(aa)(H_2O)]^+$ and anionic NO_3^- ions in aqueous solution, and that they also bind to DNA by electrostatic attraction with the negatively charged phosphate backbone of the DNA. At 20 and 40 mM NaCl, the binding constants of **4** decreased significantly, suggesting the greater weakening effect of methyl substituent at amino nitrogen than that of the methyl substituent at the α-carbon of the coordinated glycine moiety on the DNA binding affinity.

Binding with G-quadruplex

The CD spectrum of the G-quadruplex (G-4 duplex), annealed from a human telomeric 22-base oligonucleotide 5′-AG$_3$(T$_2$AG$_3$)$_3$-3′, shows two maxima at 295 and 246 nm, and a minimum at 267 nm. This has been previously established to have an anti-parallel structure

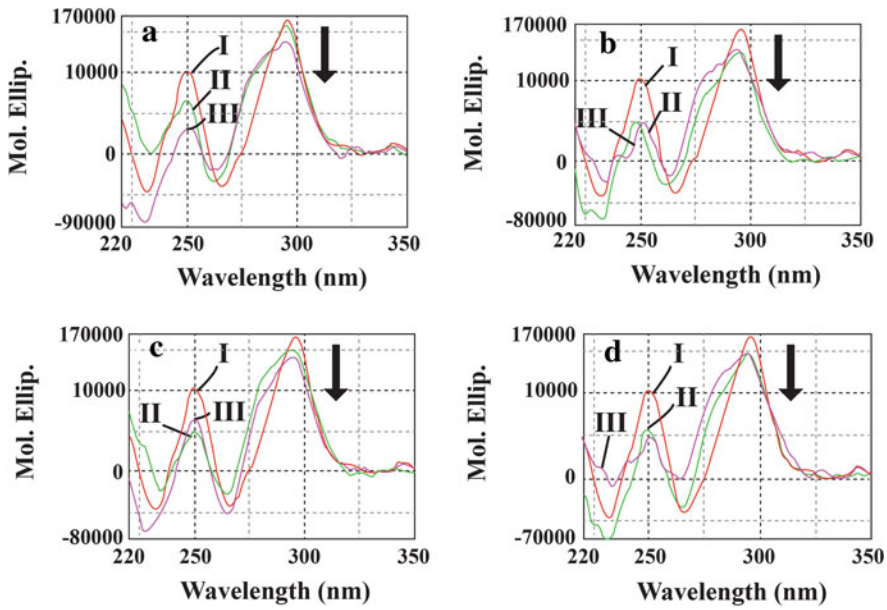

Fig. 6 Sets of CD spectra of 20 μM of G-quadruplex 5′-$AG_3(T_2AG_3)_3$-3′ in the absence and presence of different concentration of $[Cu(phen)(aa)(H_2O)]^+$ (**a** gly, **1**; **b** DL-ala, **2**; **c** C-dmg, **3**; **d** sar, **4**), and each of set of spectra **a**–**d** contains CD of G-quadruplex alone (*I*), G-quadruplex with 60 μM complex (*II*), G-quadruplex with 120 μM complex in TN buffer (*III*) (5 mM Tris, 50 mM NaCl) at pH 7.5

with basket strand orientation (Seng et al. 2009). The G-4 was titrated with increasing concentration of complexes **1**–**4** (Fig. 6). The three CD spectral peaks of the G-4 duplex did not change with the addition of each copper(II) complex, suggesting retention of the anti-parallel structure. With increasing complex concentration (60, 120 μM), the intensity of the 295 nm positive band of the G-4 duplex CD spectrum decreased, suggesting slight destabilization of the G-4 duplex (Seng et al. 2009; Nagesh and Krishnaiah 2003).

In addition to CD studies, thiazole orange quenching studies were conducted on (i) the above 22-base G-4 duplex, and (ii) a duplex (17 bp), annealed from two complementary 17 nucleotide primers, 5′-CCA GTTCGTAGTAACCC-3′ and 3′-GGTCAAGCAT-CATTGGG-5′, to find the apparent binding constants (K_{app}) of complexes **1**–**4** for these DNA structures (Seng et al. 2009). Binding constants were again calculated using a simple competitive binding model (Stern–Volmer equation) as previously described in the literature (Seng et al. 2009). The results for the G-4, duplex, and the ratio of quadruplex to duplex are shown in Table 6 and Fig. 6.

Table 6 TO quenching assay results studies of complexes **1**–**4** on G-quadruplex and duplex DNA

Complex	G-quadruplex DNA binding constants 22 G (M^{-1})	Duplex DNA binding constants 17 bp (M^{-1})	Ratio 22 G/17 bp
1	$3.4 \pm 0.13 \times 10^4$	$6.6 \pm 0.18 \times 10^3$	5.15
2	$3.7 \pm 0.16 \times 10^4$	$9.5 \pm 0.21 \times 10^3$	3.89
3	$4.5 \pm 0.19 \times 10^4$	$9.6 \pm 0.14 \times 10^3$	4.69
4	$1.0 \pm 0.09 \times 10^5$	$1.1 \pm 0.11 \times 10^4$	9.09

The variation in G-quadruplex DNA binding affinity is observed in Table 6 (and Fig. 6), in which the order of G-quadruplex DNA binding affinity of the complexes is **4** > **3** > **2** > **1**. The copper(II) complex **1**, with no methyl substituent, showed the lowest binding affinity on G-quadruplex DNA. The other complexes **2**–**4**, with methyl substituent(s), showed greater G-quadruplex DNA binding affinity. The result revealed that the G-quadruplex DNA binding affinity of **1** can be improved by incorporating methyl group(s) into the coordinated glycine. Furthermore the binding constant of **4**, compared to those of **2** and **3**, suggests greater significance of the methyl group at the amino nitrogen than at the α-carbon of the amino acid.

The 22 G-4/17 bp ratio is calculated by dividing the apparent binding constant of copper(II) complex on

22-base G-quadruplex DNA over its apparent binding constant on 17 bp duplex DNA. The 22 G-4/17 bp ratio indicates the binding selectivity of copper(II) complexes for G-quadruplex DNA sequence than for duplex DNA. However, based upon the 22 G-4/17 bp ratio, complexes **3** (22 G-4/17 bp ratio = 4.69) and **2** (22 G-4/17 bp ratio = 3.89) have lower G-quadruplex DNA selectivity than **1** (22 G-4/17 bp ratio = 5.15) while complex **4** has the greatest selectivity towards G-quadruplex DNA (22 G/17 bp ratio = 9.09) (Table 6). These results suggest that the position and number of methyl substituent in the coordinated glycine moiety modulate the G-4 binding selectivity. The above higher binding affinity for G-4 over duplex DNA is in line with the distinguishing characteristic of a molecule as potential G-4 targeting anticancer drug (Gan et al. 2011).

Topo I inhibition

Topoisomerases are proteins required for important biological processes such as DNA replication, transcription and repair, and chromatin assembly by introducing temporary DNA single-strand or double-strand break. Topo I unwind duplex DNA through transient single-strand break, resulting in a more relaxed DNA. Supercoiled plasmid DNA pBR322 is a suitable substrate to study the inhibition of Topo I as the speed of migration of the topoisomers (relaxed DNA) on the electrophoresis gel decreases with the degree of relaxation (Webb and Ebeler 2008). One unit of Topo I was able to convert all the pBR322 into full relaxed topoisomers and nicked DNA. It was observed that slower moving bands of topoisomers were formed with increasing concentration of complexes **1**–**4** (Fig. 7). These results showed that they could inhibit the Topo I and that the inhibition was concentration dependent. Visually, there seems to be no significant difference in the degree of Topo I inhibition by these complexes, suggesting no or minimal effect of the number and position of the methyl substituent in the amino acid moiety on the degree of Topo I inhibition. This Topo I inhibitory property of the above copper(II) complexes and their DNA binding specificity are similar to some anticancer organic compounds which target topoisomerases (Arjmand and Muddassir 2010; Chashoo et al. 2011; Capranico et al. 1997; Rao et al. 2007; Arimondo et al. 2006).

As a preliminary investigation into the mechanism of action of the above Topo I inhibition, we used three variations of mixing the DNA, Topo I and each of the copper(II) complexes (at 50 μM) for the Topo I inhibition assay (Fig. 8 panels a–c). The observed gel patterns (panels a–c) were distinctly different. For those experiments where copper(II) complex and Topo I were mixed first before adding DNA (Panel b), the gel images showed more intense band of fastest moving supercoiled DNA, suggesting greater inhibition of Topo I for this sequence of mixing. Prior interaction of copper(II) complexes with Topo I resulted in greater inhibition of the Topo I activity than the other modes of mixing. These results suggest that the inhibitory mechanism involves both binding of copper(II) complexes to DNA and the Topo I.

Anticancer study

The preceding discussions led us to evaluate complexes **1**–**4** and a known anticancer compound $Cu(8OHQ)_2$ (Daniel et al. 2004; Zhai et al. 2010) for their cytotoxic property in vitro against cancer nasopharyngeal cell line HK1 and normal nasopharyngeal cell line NP69. Viability-concentration curves plotted from MTT antiproliferative assay data showed that they inhibited the proliferation of the two cell lines in a dose-dependent manner when these cells were incubated with increasing concentration of test drugs (0–25 μM) for 24 h (Supplementary data: Fig. S5). The IC_{50} values of **1**–**4** for HK1 were in the range of 2.2–5.2 μM while the corresponding values for NP69 were greater than 13.0 μM (Table 7). The IC_{50} values of **2**–**4** were very similar and not significantly lower than that of **1**, suggesting no distinct effect of presence of methyl substituent(s) in glycine moiety on the antiproliferative property on HK1 cancer cells. Nevertheless, these complexes (**1**–**4**) were distinctly more antiproliferative against HK1 than NP69 by a factor of about 4 times or more than 10 times (Table 7). Cisplatin, a clinical anticancer drug with some harmful side effects, was reported to be highly cytotoxic to normal cell lines (NP69, PBMC, CCD19Lu) than NPC cell lines (SUNE1, CNE2, C666-1) (To et al. 2009; Wang et al. 2006). The known anticancer copper(II) complex that was tested, $Cu(8OHQ)_2$, was equally antiproliferative towards HK1 (IC_{50}, 2.0 μM) and NP69 (IC_{50}, 3.2 μM). Approximately 5.2–7.5 μM of **1**, 3.9–5.8 μM of **2**, 2.2–4.4 μM of **3**, and 2.2–4.8 μM

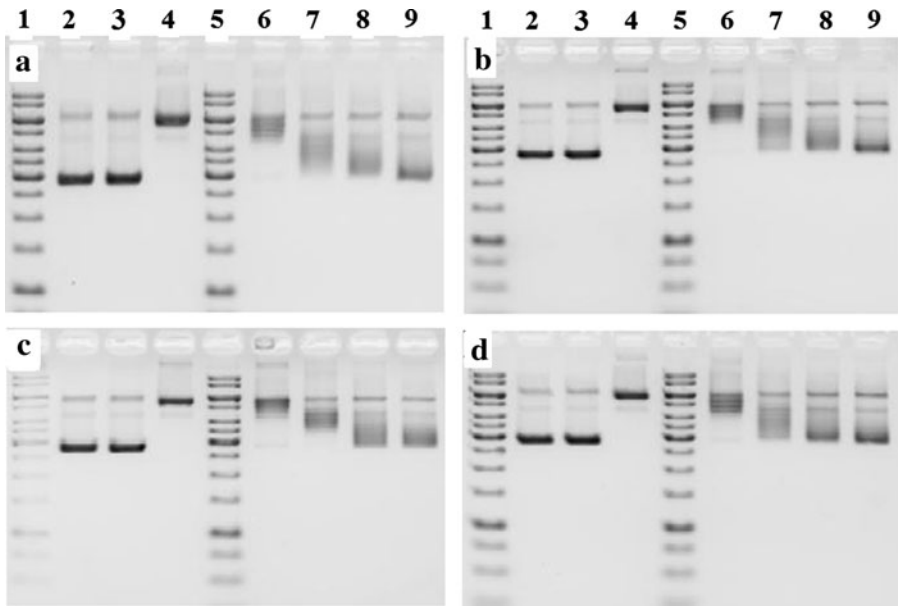

Fig. 7 Gel electrophoresis results of incubating human topoisomerase I (1 unit/21 μL) with pBR322 (0.25 μg) in the absence or presence of 5–40 μM of complexes **1**–**4** (**a** aa = gly, **1**; **b** aa = DL-ala, **2**; **c** aa = C-dmg, **3**; **d** aa = sar, **4**) where *Lane 1* & *5* gene ruler 1 Kb DNA ladder, *lane 2* DNA alone, *lane 3* DNA + 40 μM complex (control), *lane 4* DNA + 1 unit Topo I (control), *lane 6*, DNA + 5 μM complex + 1 unit Topo I, *lane 7* DNA + 10 μM complex + 1 unit Topo I, *lane 8* DNA + 20 μM complex + 1 unit Topo I, *lane 9* DNA + 40 μM complex + 1 unit Topo I

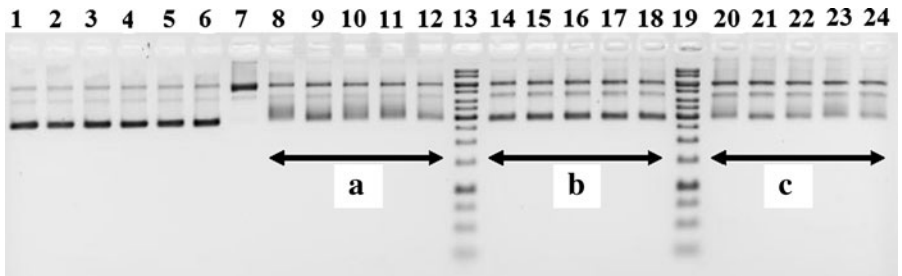

Fig. 8 Effect of sequence of mixing for the human Topo I inhibition assay. Electrophoresis results of incubating Topo I (1 unit/21 μL) with pBR322 (0.5 μg/μL) and 50 μM complexes **1**–**4**. Controls: *lane* (*L*) *1* DNA alone; DNA + 50 μL various compounds (*L2* Cu(phen)Cl_2, *L3* **1**, *L4* **3**, *L5* **2**, *L6* **4**); *L7* DNA + 1 unit Topo I. *Panel a* all three components mixed at same time; *panel b* complex + Topo I incubated for 30 min before adding DNA; and *panel c* complex + DNA incubated for 30 min before adding Topo I. Compounds and lanes: Cu(phen)Cl_2 *L8*, *L14*, *L20*; **1** *L9*, *L15*, *L21*; **3** *L10*, *L16*, *L22*; **2** *L11*, *L17*, *L23*; **4** *L12*, *L18*, *L24*

of **4** reduced the cell viability of HK1 by 50–70 % while they maintained more than 70 % of the cell viability of NP69. Thus, complexes **1**–**4** showed selectivity towards cancerous NPC over normal nasopharyngeal cells whereas both Cu(8OHQ)$_2$ and cisplatin did not.

Annexin V-FITC/PI double staining with flow cytometry was also used to compare the apoptosis induced by the 5 μM of each of the five copper(II) complexes in both cell lines (Fig. 9). Statistical analysis using Wilconxon Rank Sum test was done on the apoptosis data. The four complexes **1**–**4** induced 41–60 % apoptotic cell death in HK1 cancer cells while Cu(8OHQ)$_2$ induced 82 %. Thus, complexes **1**–**4** showed moderate activity compared to Cu(8OHQ)$_2$. It is statistically found that % apoptosis induced in normal NP69 cells by 5 μM of **1**–**4** is comparable to that in untreated cells, indicating non-toxicity of **1**–**4** towards NP69. However, 5 μM [Cu(8OHQ)$_2$] was highly cytotoxic to both NP69 (% apoptosis,

Table 7 IC_{50} values of complexes **1–4** and $[Cu(8OHQ)_2]$ for nasopharyngeal cell lines

Compound	HK1 (μM)	NP69 (μM)	Ratio NP69:HK1
$Cu(8OHQ)_2$	2.0	3.2	1.6
1	5.2	>25	>4.8
2	3.9	13.8	3.5
3	2.2	>25	>11.4
4	2.2	>25	>11.4

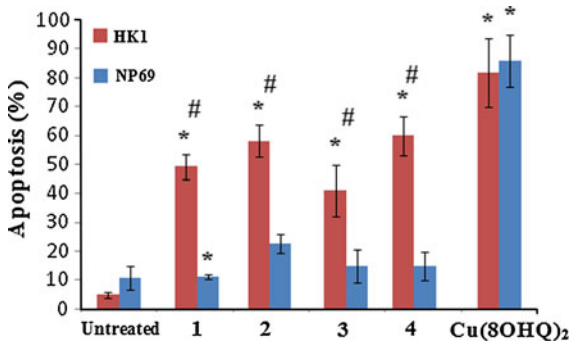

Fig. 9 % Apoptosis induced by 5 μM of complexes **1–4** and $Cu(8OHQ)_2$ in HK1 cancer cells and NP69 normal cells at 24 h incubation. $^{*}p < 0.05$ for comparing treated cells with untreated cells for the same cell line; $^{\#}p < 0.05$ for comparing treated cancer cells with treated normal cells with the same compound

88 ± 11 %) and HK1 (% apoptosis, 82 ± 12 %). In other words, $[Cu(8OHQ)_2]$ is non-cytoselective towards HK1 and NP69. Of particular interest to us was that substitution of glycine with methylated glycine to give copper(II) complexes **2–4** did not have any significant increase in their cytotoxicity towards HK1 cells compared to that of **1**.

Like other Topo I-inhibitor anticancer drugs, cytotoxic and apoptotic effects in HK1 cancer cells could result from inhibition of Topo I functions (Arjmand and Muddassir 2010; Chashoo et al. 2011). We have shown that copper(II) complexes **1–4** inhibited Topo I by either prior interaction with Topo I or initial binding to DNA. The mechanism of action of complexes **1–4** may or may not be the same as that of Topo I-inhibitor anticancer drugs. Experiments are needed to establish the mechanism via which apoptosis is induced.

Selectivity or specificity of **1–4** towards HK1 cancer cells over normal NP69 cells can be partly explained in terms of Topo I inhibition as many types of cancer cells have higher levels of Topo I than normal cells (Souza et al. 2005; Gouveris et al. 2010). Since copper(II) complexes are known to induce reactive oxygen species (ROS) and cancer cells have higher level of ROS, **1–4** could easily elevate the ROS in HK1 cells above a common "ROS threshold" which is responsible for induction of apoptosis (Wu and Hua 2007). Another mechanism involves proteasome inhibition by copper(II) complexes and this is related to the greater sensitivity of cancer cells towards proteasome inhibition (Adams 2004). Further investigations are in progress.

Conclusion

All copper(II)-phen complexes with gly or methylated glycine derivatives crystallize giving square pyramidal geometry. In aqueous solution, complexes **1–4** exists as $[Cu(phen)(aa)(H_2O)]^+$ with NO_3^- counterion and are stable up to 24 h. Replacing coordinated glycine with methylated glycine can affect the biological property of the ternary complexes. Like $[Cu(phen)(gly)(H_2O)]^+$ the other $[Cu(phen)(aa)(H_2O)]^+$ cations in **2–4** (aa = DL-ala, C-dmg, sar) bind preferentially to $ds(CG)_6$ than to $ds(AT)_6$ by a factor of two, and equally inhibit topo I. Among them, **4** (aa = sar) with methyl substituent at the amino nitrogen binds most weakly to CT-DNA (factor of 1/2). Complex **4** has the greatest binding selectivity for G-quadruplex over the corresponding duplex DNA (9×). Based on RE inhibition assay, complexes **1–4** have DNA binding selectivity, i.e. can only bind to certain sites on the DNA. In general, **3** with two methyl substituents at the α-carbon of the glycine moiety, possesses the greatest binding selectivity to both quadruplex and DNA. MTT and apoptosis assay results show that the antitumor effect of complexes **1–4** is selective towards NPC cells over corresponding normal cells. Further mechanistic studies are planned.

Acknowledgments This work is supported by MOSTI eScience grant (02-02-SF0033). We also thank the Director General of Health Malaysia for his permission to publish this article and the Director of the Institute for Medical Research for her support. Makoto Chikira acknowledges financial support from Grant-in-Aid for Science Research (No. 21550070) from the Ministry of Education, Culture, Sports, Science and Technology (MEXT), Japan. Statistical analysis on apoptosis data was done by Lee How Chinh.

References

Adams J (2004) The proteasome: a suitable antineoplastic target. Nat Rev Cancer 4:349–360

Arimondo PB, Thomas CJ, Oussedik K, Baldeyrou B, Mahieu C, Halby L, Guianvarc'h D, Lansiaux A, Hecht SM, Bailly C, Giovannangeli C (2006) Exploring the cellular activity of camptothecin-triple-helix-forming oligonucleotide conjugates. Mol Cell Biol 26:324–333

Arjmand F, Muddassir M (2010) Design and synthesis of heterobimetallic topoisomerase I and II inhibitor complexes: in vitro DNA binding, interaction with 5′-GMP and 5′-TMP and cleavage studies. J Photochem Photobiol B 101: 37–46

Beretta GL, Perego P, Zunino F (2008) Targeting topoisomerase I: molecular mechanisms and cellular determinants of response to topoisomerase I inhibitors. Expert Opin Ther Targets 12:1243–1256

Bolos C, Christidis PC, Will G, Wiehl L (1996) Synthesis and characterisation of Cu(II) complexes with the 2-acetamido-*N*-(4-methyl-2-thiazolyl) (amtz) ligand. The crystal structure of $[Cu(amtz)_2H_2O](NO_3)_2$. Inorg Chim Acta 248: 209–213

Borger DL, Fink BE, Bruette SR, Tse WC, Hedrick MP (2001) A simple, high-resolution method for establishing DNA binding affinity and sequence selectivity. J Am Chem Soc 123:5878–5891

Bruker (2009) APEX2, SAINT and SADABS. Bruker AXS Inc, Madison

Capranico G, Binaschi M, Borgnetto ME, Zunino F, Palumbo M (1997) A protein-mediated mechanism for the DNA sequence-specific action of topoisomerase II poisons. Trends Pharmacol Sci 18:323–329

Chashoo G, Singh SK, Sharma PR, Mondhe DM, Hamid A, Saxena A, Andotra SS, Shah BA, Qazi NA, Taneja SC, Saxena AK (2011) A propionyloxy derivative of 11-keto-β-boswellic acid induces apoptosis in HL-60 cells mediated through topoisomerase I & II inhibition. Chem-Biol Interact 189:60–71

Chen CH, Sigman DS (1986) Nuclease activity of 1,10-phenanthroline-copper sequence-specific targeting. Proc Natl Acad Sci USA 83:7147–7151

Chikira M (2008) DNA-fiber EPR spectroscopy as a tool to study DNA–metal complex interactions: DNA binding of hydrated Cu(II) ions and Cu(II) complexes of amino acids and peptides. J Inorg Biochem 102:1016–1024

Chikira M, Inoue M, Nagane R, Harada W, Shindo H (1997) How amino acids control the binding of Cu(II) ions to DNA (II): Effect of basic amino acid residues and the chirality on the orientation of the complexes. J Inorg Biochem 66: 131–139

Chikira M, Tomizawa YM, Fukita D, Sugizaki T, Sugawara N, Yamazaki T, Sasano A, Shindo H, Palaniandavar M, Antholine WE (2002) DNA-fiber EPR study of the orientation of Cu(II) complexes of 1,10-phenanthroline and its derivatives bound to DNA: mono(phenanthroline)-copper(II) and its ternary complexes with amino acids. J Inorg Biochem 89:163–173

Chuang N-N, Lin C-L, Chen H-K (1996) Modification of DNA topoisomerase I enzymatic activity with phosphotyrosyl protein phosphatase and alkaline phosphatase from the hepatopancreas of the shrimp *Penaeus japonicus* (Crustacea: Decapoda). Comp Biochem Physiol 114B:145–151

Daniel KG, Gupta P, Harbach RH, Guida WC, Ping Dou Q (2004) Organic copper complexes as a new class of proteasome inhibitors and apoptosis inducers in human cancer cells. Biochem Pharm 67:1139–1151

Eriksson M, Leijon M, Hiort C, Norden B, Grasuland A (1994) Binding of Δ- and Λ-$[Ru(phen)_3]^{2+}$ to $[d(CGCGATCGCG)]_2$ studied by NMR. Biochemistry 33:5031–5040

Erkkila KE, Odom DT, Barton JK (1999) Recognition and reaction of metallointercalators with DNA. Chem Rev 99:2777–2796

Francois JC, Saison-Behmoaras T, Chassignol M, Thuong NT, Helene C (1989) Sequence-targeted cleavage of single- and double-stranded DNA by oligothymidylates covalently linked to 1,10-phenanthroline. J Biol Chem 264:5891–5898

Franklin CA, Fry JV, Collins JG (1996) NMR evidence for sequence-specific DNA minor groove binding by *bis*(ethylenediamine)platinum(II). Inorg Chem 35:7541–7545

Gallori E, Vettori C, Alessio E, Vilchez FG, Vilaplana R, Orioli P, Casini A, Messori L (2000) DNA as a possible target for antitumor ruthenium(III) complexes: a spectroscopic and molecular biology study of the interactions of two representative antineoplastic ruthenium(III) complexes with DNA. Arch Biochem Biophys 376:156–162

Gan J-H, Sheng J, Huang Z (2011) Chemical and structural biology of nucleic acids and protein-nucleic acid complexes for novel drug discovery. Sci China Chem 54:3–23

Gao F, Chao H, Zhou F, Chen X, Wei Y-F, Ji L-N (2008) Synthesis, GC selective DNA binding and topoisomerase II inhibition activities of ruthenium(II) polypyridyl complex containing 11-aminopteridino[6,7-*f*][1,10]phenanthrolin-13(12*H*)-one. J Inorg Biochem 102:1050–1059

Gouveris P, Skopelitis E, Tsavaris N (2010) DNA replication—current advances. In: Seligmann H (ed) Topoisomeras I and II expression in recurrent colorectal cancer cells: a dubious matter. ISBN: 978-953-307-593-8, InTech

Halder P, Zangrando E (2010) Copper(II) α-hydroxycarboxylate complexes of bis(2-pyridylcarbonyl)amine: from mononuclear complex to one-dimensional coordination polymer. Polyhedron 29:434–440

Ikotun OF, Higbee EM, Ouellette W, Doyle RP (2009) Pyrophosphate-bridged complexes with picomolar toxicity. J Inorg Biochem 103:1254–1264

Kikuta E, Matsubara R, Katsube N, Koike T, Kimura E (2000) Selective recognition of consecutive G sequence in double-stranded DNA by a zinc(II)–macrocyclic tetraamine complex appended with an anthraquinone. J Inorg Biochem 82:239–249

Kostova I (2006) Platinum complexes as anticancer agents: recent patents on anti-drugs. Cancer Drug Discov 1:1–22

Krotz AH, Kuo LY, Shields TP, Barton JK (1993) DNA recognition by rhodium(III) polyamine intercalators: considerations of hydrogen bonding and van der Waals interactions. J Am Chem Soc 115:3877–3882

Kumar Singh S, Joshi S, Ranjan Singh A, Saxena JK, Pandey DS (2007) DNA binding and topoisomerase II inhibitory activity of water-soluble ruthenium(II) and rhodium(III) complexes. Inorg Chem 46:10869–10876

Meistermann I, Moreno V, Prieto MJ, Moldrheim E, Sletten E, Khalid S, Rodger PM, Peberdy JC, Isaac CJ, Rodger A, Hannon MJ (2002) Intramolecular DNA coiling mediated by metallo-supramolecular cylinders: differential binding of P and M helical enantiomers. Proc Natl Acad Sci USA 99:5069–5074

Mestre B, Pitié M, Loup C, Claparols C, Pratviel G, Meunier B (1997) Influence of the nature of the porphyrin ligand on the nuclease activity of metalloporphyrin-oligonucleotide conjugates designed with cationic, hydrophobic or anionic metalloporphyrins. Nucl Acids Res 25:1022–1027

Miller KM, Rodriguez R (2011) G-quadruplexes: selective DNA targeting for cancer therapeutics. Expert Rev Clin Pharmacol 4:139–142

Monchaud D, Allain C, Bertrand H, Smargiasso N, Rosu F, Gabelica V, De Cian A, Mergny J-L, Teulade-Fichou M-P (2008) Ligands playing musical chairs with G-quadruplex DNA: a rapid and simple displacement assay for identifying selective G-quadruplex binders. Biochimie 90:1207–1223

Nagesh N, Krishnaiah A (2003) A comparative study on the interaction of acridine and synthetic *bis*-acridine with G-quadruplex structure. J Biochem Biophys Methods 57: 65–74

Nakabayashi Y, Iwamoto N, Inada H, Yamauchi O (2006) DNA-binding properties of flexible diamine bridged dinuclear ruthenium(II)-2,2′-bipyridine complexes. Inorg Chem Commun 9:1033–1036

Neidle S (2010) Human telomeric G-quadruplex: the current status of telomeric G-quadruplexes as therapeutic targets in human cancer. FEBS J 277:1118–1125

Patra AK, Bhowmick T, Ramakumar S, Chakravarty AR (2007) Metal-based netropsin mimics showing AT-selective DNA binding and DNA cleavage activity at red light. Inorg Chem 46:9030–9032

Pommier Y (2006) Topoisomerase I inhibitors: camptothecins and beyond. Nat Rev Cancer 6:789–802

Rajendiran V, Murali M, Suresh E, Palaniandavar M, Periasamy VS, Akbarsha MA (2008) Non-covalent DNA binding and cytotoxicity of certain mixed-ligand ruthenium(II) complexes of 2,2′-dipyridylamine and diimines. Dalton Trans 16:2157–2170

Rajendran A, Nair BU (2006) Unprecedented dual binding behaviour of acridine group of dye: a combined experimental and theoretical investigation for the development of anticancer chemotherapeutic agents. Biochim Biophys Acta 1760:1794–1801

Rao VA, Agama K, Holbeck S, Pommier Y, Batracylin (NSC 320846) (2007) A dual inhibitor of DNA topoisomerases I and II induces histone gamma-H2AX as a biomarker of DNA damage. Cancer Res 67:9971–9979

Reichmann RE, Rice SA, Thomas CA, Doty P (1954) A further examination of the molecular weight of desoxypentose nucleic acid. J Am Chem Soc 76:3047–3053

Rothenberg ML (1997) Topoisomerase I inhibitors: review and update. Ann Oncol 8:837–855

Ruíz P, Ortiz R, Perelló L, Alzuet G, González-Álvarez M, Liu-González M, Sanz-Ruíz F (2007) Synthesis, structure and nuclease properties of several binary and ternary complexes of copper(II) with norfloxacin and 1,10-phenanthroline. J Biol Inorg Chem 101:831–840

Rupesh KR, Deepalatha S, Krishnaveni M, Venkatesan R, Jayachandran S (2006) Synthesis, characterization and in vitro biological activity studies of Cu–M (M = Cu^{2+}, Co^{2+}, Ni^{2+}, Mn^{2+}, Zn^{2+}) bimetallic complexes. Eur J Med Chem 41:1494–1503

Seng HL (2010) Duplex and G-quadruplex DNA binding, nucleolytic property and topoisomerase I inhibition by different series of metal(II) complexes. Dissertation, Universiti Tunku Abdul Rahman, Kampar

Seng HL, Von ST, Tan KW, Maah MJ, Ng SW, Raja Abd Rahman RNZ, Caracelli I, Ng CH (2009) Crystal structure, DNA binding studies, nucleolytic property and topoisomerase I inhibition of zinc complex with 1,10-phenanthroline and 3-methyl-picolinic acid. Biometals 23:99–118

Sheldrick GM (1996) SADABS. University of Göttingen, Germany

Sheldrick GM (1997a) SHELXS 97 program for crystal structure solution. University of Göttingen, Göttingen

Sheldrick GM (1997b) SHELXL-97 program for crystal structure refinement. University of Göttingen, Göttingen

Sheldrick GM (2008) A short history of SHELX. Acta Cryst A 64:112

Sitlani A, Barton JK (1994) Sequence-specific recognition of DNA by phenanthrenequinone diimine complexes of rhodium(III): importance of steric and van der Waals interactions. Biochemistry 33:12100–12108

Sitlani A, Dupureur CM, Barton JK (1993) Enantiospecific palindromic recognition of 5′-d(CTCTAGAG)-3′ by a novel rhodium intercalator:analogies to a DNA-binding protein. J Am Chem Soc 115:12589–12590

Snow AM, Sheardy RD (2001) Locating cobalt-binding sites on DNA using restriction endonucleases. Methods Enzymol 340:519–528

Souza V, Dong YB, Zhou HS, Zacharias W, McMasters KM (2005) SW-620 cells treated with topoisomerase I inhibitor SN-38: gene expression profiling. J Transl Med 44:1–7

Sunami S, Nishimura T, Nishimura I, Ito S, Arakawa H, Ohkubo M (2009) Synthesis and biological activities of topoisomerase I inhibitors, 6-arylmethylamino analogues of edotecarin. J Med Chem 52:3225–3237

Sung FL, Poon TCW, Hui EP, Ma BBY, Liong E, To KF, Huang DPWS, Chan ATC (2005) Antitumor effect and enhancement of cytotoxic drug activity by cetuximab in nasopharyngeal carcinoma cells. In Vivo 19:237–246

Tan KW, Ng CH, Mohd Jamil M, Ng SW (2008) Chlorido(2-methyl-4-oxo-4*H*-pyran-3-olato-κ^2O^3,O^4)(1,10-phenanthroline-κ^2N,N')copper(II). Acta Cryst E64:m1104

Tan J, Jun L, Wang B (2010) From GC-rich DNA binding to the repression of survivin gene for quercetin nickel(II) complex: implications for cancer therapy. Biometals 23:1075–1084

Teicher BA (2008) Next generation topoisomerase I inhibitors: rationale and biomarker strategies. Biochem Pharmacol 75:1262–1271

To YF, Raymond Sun W-Y, Chen Y, Vera Chan S-F, Yu W-Y, Paul Tam K-H, Che C-M, Steve Lin C-L (2009) Gold(III) porphyrin complex is more potent than cisplatin in inhibiting growth of nasopharyngeal carcinoma in vitro and in vivo. Int J Cancer 124:1971–1979

Vermorken JB, Trigo J, Hitt R, Koralewski P, Diaz-Rubio E, Rolland F, Knecht R, Amellal N, Schueler A, Baselga J

(2007) Open label, uncontrolled, multicenter phase II study to evaluate the efficacy and toxicity of cetuximab as a single agent in patients with recurrent and/or metastatic squamous cell carcinoma of the head and neck who failed to respond to platinum-based therapy. J Clin Oncol 25: 2171–2177

Wang X, Wang L-K, Kinsbury WD, Johnson RK, Hecht SM (1998) Differential effects of camptothecin derivatives on topoisomerase I-mediated DNA structure modification. Biochemistry 37:9399–9408

Wang Y, He Q-Y, Che C-M, Chiu J-F (2006) Proteomic characterization of cytotoxic mechanism of gold(III) porphyrin 1a, a potential anticancer drug. Proteomics 6:131–142

Webb MR, Ebeler SE (2008) Anthocyanin interactions with DNA: intercalation topoisomerase I inhibition and oxidative reactions. J Food Biochem 32:576–596

Wheate NJ, Collins JG (2000) A ^{1}H NMR study of the oligonucleotide binding of [(en)Pt(μ-dpzm)$_2$Pt(en)]Cl$_4$. J Inorg Biochem 78:313–320

Wu XJ, Hua X (2007) Selective killing of cancer cells by a cruciferous vegetable derived pro-oxidant compound. Cancer Biol Ther 6:646–647

Wu Y, Chen H, Yang P, Xiong Z (2005) Racemic D,L-[Co(phen)$_2$dpq]$^{3+}$–DNA interactions: investigation into the basis for minor-groove binding and recognition. J Inorg Biochem 99:1126–1134

Xu L, Liao G-L, Chen X, Zhao C-Y, Chao H, Ji L-N (2010) Trinuclear Ru(II) polypyridyl complexes as human telomeric quadruplex DNA stabilizers. Inorg Chem Commun 13:1050–1053

Zeglis BM, Pierre VC, Barton JK (2007) Metallo-intercalators and metallo-insertors. Chem Commun 44:4565–4579

Zhai S, Yang L, Cindy Cui Q, Sun Y, Ping Dou Q, Yan B (2010) Tumor cellular proteasome inhibition and growth suppression by 8-hydroxyquinoline and clioquinol requires their capabilities to bind copper and transport copper into cells. J Biol Inorg Chem 15:259–269

Zhang S, Zhou J (2008) Ternary copper(II) complex of 1,10-phenanthroline and L-glycine: crystal structure and interaction with DNA. J Coord Chem 61:2488–2498